Inhomogeneous Shadowing Effects on J/ψ Production in dA Collisions

S. R. Klein[1] and R. Vogt[1,2]
[1] *Nuclear Science Division, Lawrence Berkeley National Laboratory, Berkeley, CA 94720, USA*
[2] *Physics Department, University of California, Davis, CA 95616, USA*

Abstract

We study the effect of spatially homogeneous and inhomogeneous shadowing on J/ψ production in deuterium-nucleus collisions. We discuss how the shadowing and its spatial dependence can be measured by comparing central and peripheral dA collisions. These event classes may be selected by using gray protons from heavy ion breakup and events where the proton or neutron in the deuterium does not interact. We find that inhomogenous shadowing has a significant effect on central dA collisions, larger than expected in central AA collisions. Results are presented for dAu collisions at $\sqrt{s_{NN}} = 200$ GeV and dPb collisions at $\sqrt{s_{NN}} = 6.2$ TeV.

I. INTRODUCTION

The nuclear quark and antiquark distributions have been probed through deep inelastic scattering (DIS) of leptons and neutrinos from nuclei. These experiments showed that parton densities in free protons are modified when bound in the nucleus [1]. This modification, referred to collectively as shadowing, depends on the parton momentum fraction x and the square of the momentum transfer, Q^2. Most models of shadowing predict that the modification should vary depending on position within the nucleus [2]. Most DIS experiments have been insensitive to this position dependence. However, some spatial inhomogeneity has been observed in νN scattering in emulsion [3].

Deuterium-nucleus collisions at heavy ion colliders offer a way to measure the structure functions of heavy nuclei at higher energies, hence lower x and higher Q^2 than currently possible with fixed target DIS experiments. In addition, dA collisions are more sensitive to the gluon distributions in nuclei than DIS. These dA collisions are preferred over pA collisions for technical reasons - the two beams have similar charge Z to mass A ratios, simplifying the magnetic optics. While shadowing measurements in pA and dA interactions have been discussed previously [4], the spatial dependence remains unexplored. This dependence is of great interest both as a probe of the shadowing mechanism and as an important input to studies of high energy AA collisions.

In this letter, we show that dA collisions can be used to study the spatial dependence of nuclear gluon shadowing. We consider two concrete examples: dAu interactions at $\sqrt{s_{NN}} =$

200 GeV at RHIC and 6.2 TeV dPb interactions at the LHC.

We choose the J/ψ as a specific example since it has already been observed in pp and Au+Au interactions at RHIC [5]. Because we focus on the magnitude of the shadowing effect, we do not include nuclear absorption or transverse momentum, p_T, broadening in our calculations. Our techniques are applicable to other hard probes such as Υ, open charm and bottom quarks, Drell-Yan dileptons, jets, and dijets, and, at the LHC, $W^{\pm}$ and Z^0 production. With a variety of probes, both quark and gluon shadowing can be measured over a wide range of x and Q^2.

Our calculations employ the color evaporation model (CEM) which treats all charmonium production identically to $c\overline{c}$ production below the $D\overline{D}$ threshold, neglecting color and spin. The leading order (LO) rapidity distributions of J/ψ's produced in dA collisions at impact parameter b is

$$\frac{d\sigma}{dy\,d^2b\,d^2r} = 2F_{J/\psi}K_{\rm th}\int dz\,dz'\int_{2m_c}^{2m_D} M\,dM\left\{F_g^d(x_1,Q^2,\vec{r},z)F_g^A(x_2,Q^2,\vec{b}-\vec{r},z')\frac{\sigma_{gg}(Q^2)}{M^2}\right. \quad (1)$$

$$\left. + \sum_{q=u,d,s}[F_q^d(x_1,Q^2,\vec{r},z)F_{\overline{q}}^A(x_2,Q^2,\vec{b}-\vec{r},z') + F_{\overline{q}}^d(x_1,Q^2,\vec{r},z)F_q^A(x_2,Q^2,\vec{b}-\vec{r},z')]\frac{\sigma_{q\overline{q}}(Q^2)}{M^2}\right\} .$$

The partonic $c\overline{c}$ cross sections are defined in Ref. [6], $M^2 = x_1x_2s$ and $x_{1,2} = (M/\sqrt{s_{NN}})\exp(\pm y) \approx (m_{J/\psi}/\sqrt{s_{NN}})\exp(\pm y)$ where $m_{J/\psi}$ is the J/ψ mass. The fraction of $c\overline{c}$ pairs below the $D\overline{D}$ threshold that become J/ψ's, $F_{J/\psi}$, is fixed at next-to-leading order (NLO) [7]. Both this fraction and the theoretical K factor, $K_{\rm th}$, drop out of the ratios. We use $m_c = 1.2$ GeV and $Q = M$ [7].

We assume that the nuclear parton densities, F_i^A, are the product of the nucleon density in the nucleus, $\rho_A(s)$, the nucleon parton density, $f_i^N(x,Q^2)$, and a shadowing ratio, $S_{\rm P,S}^i(A,x,Q^2,\vec{r},z)$, where $\vec{r}$ and z are the transverse and longitudinal location of the parton in position space. The first subscript, P, refers to the choice of shadowing parameterization, while the second, S, refers to the spatial dependence. Most available shadowing parameterizations ignore effects in deuterium. However, we take the proton and neutron numbers of both nuclei into account. Thus,

$$F_i^d(x,Q^2,\vec{r},z) = \rho_d(s)f_i^N(x,Q^2) \quad (2)$$

$$F_j^A(x,Q^2,\vec{b}-\vec{r},z') = \rho_A(s')S_{\rm P,S}^j(A,x,Q^2,\vec{b}-\vec{r},z')f_j^N(x,Q^2) , \quad (3)$$

where $s = \sqrt{r^2+z^2}$ and $s' = \sqrt{|\vec{b}-\vec{r}|^2+z'^2}$. In the absence of nuclear modifications, $S_{\rm P,S}^i(A,x,Q^2,\vec{r},z) \equiv 1$. The nucleon densities of the heavy nucleus are assumed to be Woods-Saxon distributions with $R_{\rm Au} = 6.38$ fm and $R_{\rm Pb} = 6.62$ fm [8]. We use the Hulthen wave function [9] to calculate the deuteron density distribution. The densities are normalized so that $\int d^2r\,dz\,\rho_A(s) = A$. We employ the MRST LO parton densities [10] for the free nucleon.

We have chosen two shadowing parameterizations which cover extremes of gluon shadowing at low x. The Eskola *et al.* parameterization, EKS98, is based on the GRV LO [11] parton densities. Valence quark shadowing is identical for u and d quarks. Likewise, the shadowing of $\overline{u}$ and $\overline{d}$ quarks are identical. Shadowing of the heavier flavor sea, $\overline{s}$ and higher, is calculated separately. The shadowing ratios for each parton type are evolved to LO for $1.5 < Q < 100$ GeV and are valid for $x \geq 10^{-6}$ [12,13]. Interpolation in nuclear mass

number allows results to be obtained for any input A. The parameterization by Frankfurt, Guzey and Strikman, FGS, combines Gribov theory with hard diffraction [14]. It is based on the CTEQ5M [15] parton densities and evolves each parton species separately to NLO for $2 < Q < 100$ GeV. Although the given x range is $10^{-5} < x < 0.95$, the sea quark and gluon ratios are unity for $x > 0.2$. The EKS98 valence quark shadowing ratios are used as input. The parameterization is available for $A = 16$, 40, 110 and 206. We use the $A = 206$ values for both Au and Pb.

Figure 1 compares the homogeneous ratios, $S_{\rm EKS98}$ and $S_{\rm FGS}$ for $Q = 2m_c$. The FGS calculation predicts far more shadowing at small x and larger antishadowing at $x \sim 0.1$. The difference is especially large for gluons.

We have calculated homogeneous shadowing effects on J/ψ production at NLO. However, the additional integrals required to calculate inhomogeneous effects at NLO lead to significant numerical difficulties. Therefore we have compared the LO and NLO calculations of homogeneous shadowing in pAu interactions at $\sqrt{s_{NN}} = 200$ GeV using the EKS98 parameterization to verify that the results are essentially identical.

Some differences may arise from the use of the MRST HO [16] parton densities in the NLO code while the LO calculation uses the MRST LO [10] parton densities. In addition, at NLO, qg scattering gives a small contribution. The NLO and LO ratios agree well because J/ψ production is dominated by gluons for $x_F < 0.6$, corresponding to $|y| < 3$ at RHIC and $|y| < 6.4$ at the LHC. Thus the LO calculation should reproduce the essential effects of inhomogeneous shadowing.

Shadowing is not the only nuclear effect on J/ψ production. Broadening of the p_T distributions, observed in fixed-target measurements [17], arises from multiple scattering of the initial-state partons [18] and does not affect the total cross section. Thus, a p_T-integrated measurement should be insensitive to this effect. Nucleon absorption depends on the J/ψ production mechanism [19]. Absorption is likely to increase at large negative rapidities where the J/ψ may hadronize inside the target. However, this region is outside the rapidity coverage of the present detector configurations.

We now turn to the spatial dependence of the shadowing. We use two different parameterizations for inhomogeneous shadowing in AA collisions [2,20–22]. The first, $S_{\rm P,WS}$, assumes that shadowing is proportional to the local density, $\rho(s)$,

$$S^i_{\rm P,WS}(A,x,Q^2,\vec{r},z) = 1 + N_{\rm WS}[S^i_{\rm P}(A,x,Q^2) - 1]\frac{\rho_A(s)}{\rho_0} \ , \qquad (4)$$

where ρ_0 is the central density and $N_{\rm WS}$ is chosen so that $(1/A)\int d^2r dz \rho_A(s) S^i_{\rm P,WS} = S^i_{\rm P}$. When $s \gg R_A$, the nucleons behave as free particles while in the center of the nucleus, the modifications are larger than the average value $S^i_{\rm P}$.

If, on the other hand, shadowing stems from multiple interactions of the incident parton [23], parton-parton interactions are spread longitudinally over the coherence length, $l_c = 1/2m_N x$, where m_N is the nucleon mass [24]. For $x < 0.016$, $l_c > R_A$ for any A. The interaction is then delocalized over the entire trajectory so that the incident parton interacts coherently with all the target partons along its path length. At large x, $l_c \ll R_A$ and shadowing is proportional to the local density, as above. The numerical differences between the two models are small and the available data [3] cannot tell the difference. However, the both spatial dependencies predict significant differences from the homogenous shadowing.

Because of the difficulty of matching shadowing at large and small x while conserving baryon number and momentum, we consider the small and large x limits separately. This matching is necessary because, for $y < -2$ at RHIC, $l_c < R_{\rm Au}$. This regime is measurable in the PHENIX muon spectrometers [5]. Equation (4) corresponds to the large x limit. When $l_c \gg R_A$, the spatial dependence may be parameterized as

$$S^i_{{\rm P},\rho}(A,x,Q^2,\vec{r},z) = 1 + N_\rho(S^i_{\rm P}(A,x,Q^2) - 1)\frac{\int dz \rho_A(\vec{r},z)}{\int dz \rho_A(0,z)} \ . \tag{5}$$

The integral over z includes the material traversed by the incident nucleon. The normalization requires $(1/A)\int d^2r dz \rho_A(s) S^i_{{\rm P},\rho} = S^i_{\rm P}$. We find $N_\rho > N_{\rm WS}$.

Figure 2 shows the ratios of J/ψ production per nucleon in dA interactions with and without shadowing as a function of rapidity at RHIC ($\sqrt{s_{NN}}$ = 200 GeV) and the LHC ($\sqrt{s_{NN}} = 6.2$ TeV). These ratios are essentially equivalent to the dA per nucleon to pp ratio at the same energy since isospin has a negligible effect on J/ψ production.

We consider central ($b < 0.2R_A$) and peripheral ($0.9R_A < b < 1.1R_A$) collisions. Central collisions can be selected by choosing events with a large number of 'grey protons' which move with approximately the beam rapidity. Grey protons, slow in the target rest frame, are ejected from the heavy nucleus in the collision. The name originates from the appearance of their tracks in nuclear emulsion. Their momentum must be larger than the Fermi momentum of the target. The number of grey protons is related to the number of NN collisions, ν, which is closely related to the impact parameter. Thus the number of grey protons could be used to select quite central collisions. This technique was used in the νA study of inhomogeneity [3] as well as in lower energy pA studies [25]. In the multiple interaction picture, shadowing should be directly proportional to ν.

At a heavy ion collider, grey protons can be detected in a forward proton calorimeter (FPC). Neutrons detected in a zero degree calorimeter (ZDC), could also be used, although, because of the transverse momentum, the acceptance would be limited.

Peripheral collisions could be selected using two criteria. Selecting events with a small number of grey protons preferentially chooses a small number of interactions. It is also possible to select events where only one of the nucleons in the deuteron interacts while the other is unaffected. Non-interacting nucleons can be detected in FPCs or ZDCs. In these NA collisions, the interacting deuterium nucleon is usually near the surface of the heavy ion, so that $b > R_A - 2$ fm. However, since the deuteron has a significant density even at large distances, not all single-nucleon interactions are very peripheral.

In dA collisions, the difference between one or two deuterium participants in the interaction is significant. This complication can be partly controlled by detecting the non-interacting nucleon in forward calorimeters. It can be further controlled by studying the J/ψ rapidity distribution. The rapidity, $y = y_c$, at which shadowing disappears, $S^i_{\rm P} \to 1$, could be used as a calibration point. If the deuterium comes from negative rapidity, J/ψ production at negative y occurs via small x partons in the deuteron. The rapidity distribution ratios are essentially mirror images of the shadowing parameterizations in Fig. 1. Since $S^g_{\rm P} \approx 1$ at $x \approx 0.025$, $y_c \approx -0.2$ at RHIC and -3.2 at the LHC.

The J/ψ rate at $y = y_c$ could be used to normalize the cross sections in different impact parameter classes, necessary if the absolute efficiency of cuts on grey protons is difficult to assess. The point $y = y_c$ could also be used to normalize the dA data to pp data at the

same energy, providing a direct measurement of shadowing since higher order corrections unrelated to shadowing cancel out in the ratio. Although y_c may not be perfectly known, the exact value of y_c is not important since a slight error will only affect the absolute value of the ratio. If the J/ψ absorption is independent of rapidity in the region of interest, any impact parameter dependence in the absorption correction will likewise only affect the absolute value of the ratio, not the rapidity dependence.

In Fig. 2, the homogeneous results are indicated by the solid (EKS98) and dashed (FGS) lines. The inhomogeneous results are indicated by the symbols: $S_{\mathrm{P,WS}}$ is indicated by the circles and squares while $S_{\mathrm{P},\rho}$ is given by the x's and diamonds. It is obvious that $S_{\mathrm{P},\rho}$ has a stronger spatial dependence. The overall inhomogeneity is larger for $S_{\mathrm{FGS,S}}$ as may be expected.

In central collisions, the inhomogeneous shadowing is stronger. The stronger the homogeneous shadowing, the larger the inhomogeneity. In peripheral collisions, the inhomogenous effects are somewhat weaker than the homogenous results but some shadowing is still present. Shadowing persists in part because the density in a heavy nucleus is large and approximately constant except close to the surface and partly because the deuteron wave function has a non-zero amplitude at quite large distances. These tails lead to some shadowing effects even at very large impact parameters. We have verified that the impact-parameter integrated results are identical to the homogenous results, as expected.

In dA collisions, the rapidity-dependent inhomogeneity is somewhat stronger than that predicted for AA collisions [2]. Central dA collisions are confined to the center of the target nucleus, where the effect is stronger, while central AA collisions include both central and peripheral nucleon-nucleon interactions.

Since the proton is effectively a point particle, the predicted inhomogeneity is even stronger for pA collisions. However, in pA collisions, the impact parameter determination would be considerably more difficult due to the reduced number of NN interactions.

At RHIC, the STAR and PHENIX electromagnetic calorimetry and the PHENIX muon arms cover most of the rapidity range required to compare the shadowing and antishadowing regions. Both detectors should be able to study most of the J/ψ p_T spectrum. A cut on minimum lepton p_T might reduce the sensitivity to low p_T J/ψs. A cut on J/ψ p_T would increase the x and Q^2 values probed at a given y, allowing cross-checks on the shadowing data. The 'cost' of this cut would be some sensitivity to p_T broadening.

At the LHC, the very high energy moves the antishadowing region out of the reach of any planned lepton coverage. Only the low x and transition regions might be observable at low p_T. Together, the ALICE and CMS detectors cover most of the region $-2.4 < y < 4.0$ and should be able to clearly distinguish both the homogeneous effect and the gross features of the inhomogeneity. If both dA and Ad collisions were studied, the y range would be extended down to -4.0, covering the transition region. A p_T cut on the J/ψ would increase the x and Q^2 values, perhaps moving the antishadowing region within reach. The Υ has a very similar production mechanism, but would probe larger x and Q^2 values, and should be sensitive to antishadowing at large $|y|$.

In conclusion, we have shown how nuclear shadowing can be measured with J/ψ production in dA collisions. The J/ψ rapidity is related to the momentum fraction of the target parton, allowing for measurement of the x dependence of shadowing. By selecting events with different numbers of grey protons and/or a surviving spectator nucleon from the

deuteron, it is possible to study the spatial dependence of shadowing. In all of the models considered, the inhomogeneity is large enough to be easily measured. Although we have focused on J/ψ, the same approach should apply to other hard probes.

We thank K.J. Eskola and V. Guzey for providing the shadowing routines and for discussions. This work was supported in part by the Division of Nuclear Physics of the Office of High Energy and Nuclear Physics of the U.S. Department of Energy under Contract Number DE-AC03-76SF00098.

REFERENCES

[1] J.J. Aubert *et al.*, Nucl. Phys. **B293**, 740 (1987); M. Arneodo, Phys. Rep. **240**, 301 (1994).

[2] V. Emel'yanov, A. Khodinov, S.R. Klein and R. Vogt, Phys. Rev. C **61**, 044904 (2000).

[3] T. Kitagaki *et al.*, Phys. Lett. **B214**, 281 (1988).

[4] See *e.g.* K.J. Eskola, V.J. Kolhinen and R. Vogt, Nucl. Phys. **A696**, 729 (2001); S. Liuti and R. Vogt, Phys. Rev. **C51**, 2244 (1995).

[5] A.D. Frawley *et al.* (PHENIX Collaboration), in proceedings of Quark Matter '02, Nantes, France, July, 2002 [arXiv:nucl-ex/0210013].

[6] B.L. Combridge, Nucl. Phys. **B151**, 429 (1979).

[7] R.V. Gavai, D. Kharzeev, H. Satz, G. Schuler, K. Sridhar and R. Vogt, Int. J. Mod. Phys. **A10**, 3043 (1995); G.A. Schuler and R. Vogt, Phys. Lett. **B387**, 181 (1996).

[8] C.W. deJager, H. deVries, and C. deVries, Atomic Data and Nuclear Data Tables **14**, 485 (1974).

[9] D. Kharzeev, E.M. Levin and M. Nardi, hep-ph/0212316; L. Hulthen and M. Sagawara, in *Handbüch der Physik*, **39** (1957).

[10] A.D. Martin, R.G. Roberts, and W.J. Stirling, and R.S. Thorne, Phys. Lett. **B443**, 301 (1998).

[11] M. Glück, E. Reya, and A. Vogt, Z. Phys. **C53**, 127 (1992).

[12] K.J. Eskola, V.J. Kolhinen and P.V. Ruuskanen, Nucl. Phys. **B535**, 351 (1998).

[13] K.J. Eskola, V.J. Kolhinen and C.A. Salgado, Eur. Phys. J. **C9**, 61 (1999).

[14] L. Frankfurt, V. Guzey and M. Strikman, arXiv:hep-ph/0303022.

[15] H.L. Lai *et al.*, Eur. Phys. J. **C12**, 375 (2000).

[16] A.D. Martin, R.G. Roberts, and W.J. Stirling, and R.S. Thorne, Eur. Phys. J. **C4**, 463 (1998).

[17] J. Badier *et al.* [NA3 Collaboration], Z. Phys. C **20**, 101 (1983); D.M. Alde *et al.* [E772 Collaboration], Phys. Rev. Lett. **66**, 2285 (1991).

[18] P. Hoyer and S. Peigne, Phys. Rev. D **57**, 1864 (1998) and references therein.

[19] R. Vogt, Phys. Rev. **C61**, 035203 (2000); Nucl. Phys. A **700**, 539 (2002).

[20] V. Emel'yanov, A. Khodinov, S.R. Klein and R. Vogt, Phys. Rev. **C56**, 2726 (1997).

[21] V. Emel'yanov, A. Khodinov, S.R. Klein and R. Vogt, Phys. Rev. Lett. **81**, 1801 (1998).

[22] V. Emel'yanov, A. Khodinov, S.R. Klein and R. Vogt, Phys. Rev. C **59**, R1860 (1999).

[23] A.L. Ayala, M.B. Gay Ducati and E.M. Levin, Nucl. Phys. **B493**, 305 (1997).

[24] Z. Huang, H. Jung Lu and I. Sarcevic, Nucl. Phys. **A637**, 79 (1998).

[25] I. Chemakin *et al.*, Phys. Rev. **C60**, 024902 (1999).

[26] P. Giubellino, for the ALICE Collaboration, Eur. Phys.J. direct **C4S1**, 5 (2002); CMS Collaboration, Technical Proposal, CERN-LHCC-94-38, 1994.

FIGURES

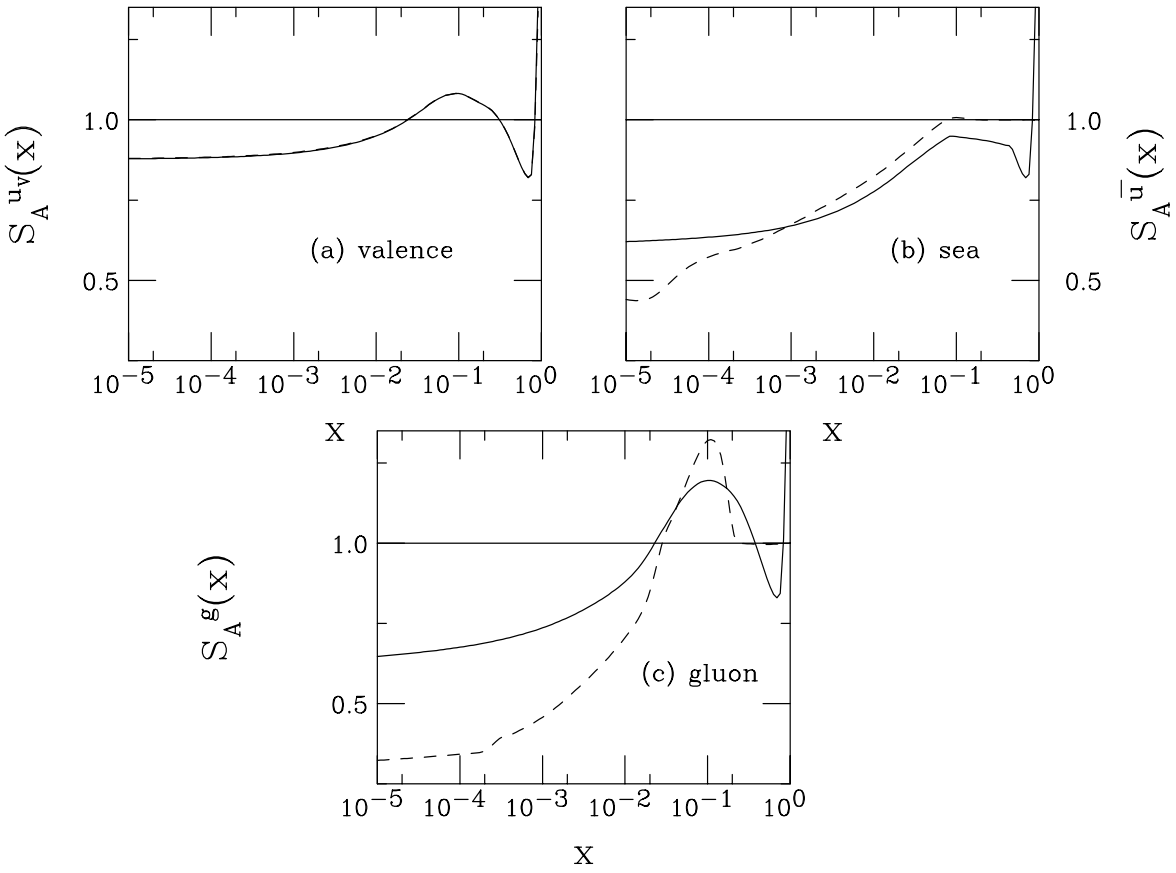

FIG. 1. The EKS98 and FGS shadowing parameterizations are compared at the scale $\mu = 2m_c = 2.4$ GeV. The solid curves are the EKS98 parameterization, the dashed, FGS.

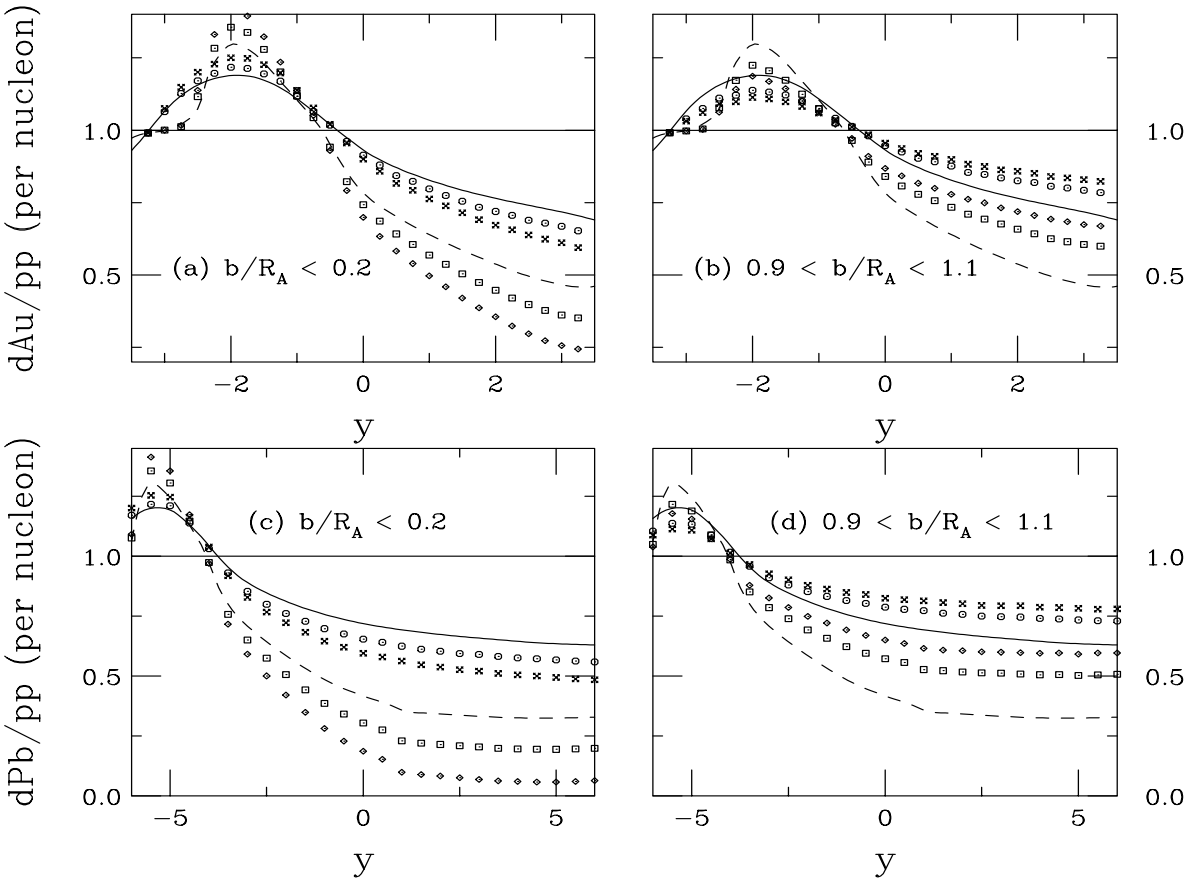

FIG. 2. The J/ψ shadowing ratio for (a and b) 200 GeV AuAu collisions and (b) 6.2 TeV PbPb collisions as a function of rapidity. The results are shown for the EKS98 (solid line for homogeneous shadowing, circles and x's for $S^i_{\mathrm{EKS98,WS}}$ and $S^i_{\mathrm{EKS98},\rho}$ respectively) and FGS (dashed line for homogeneous shadowing, squares and diamonds for $S^i_{\mathrm{FGS,WS}}$ and $S^i_{\mathrm{FGS},\rho}$ respectively). The impact parameter bins are (a) and (c) $b/R_A < 0.2$, (b) and (d) $0.9 < b/2R_A < 1.1$, and (c) all b.